VCSEL with reticular electrode and larger emitting aperture and its optoelectronic characteristics

Yuan Feng (冯 源)*, Lifeng Hou (侯立峰), Yongqin Hao (郝永芹), Changling Yan (晏长岭), Yingjie Zhao (赵英杰), Yuxia Wang (王玉霞), and Jingchang Zhong (钟景昌)

National Key Laboratory on High Power Semiconductor Lasers, Changchun University of Science and Technology, Changchun 130022, China

**E-mail: fengyuan_1224@163.com*

Received March 1, 2010

The enlargement of the emitting aperture is usually one of the important methods of increasing vertical-cavity surface-emitting laser (VCSEL) optical output power. However, in a VCSEL with a larger aperture, the inhomogeneity in the injected current often causes inhomogeneous or even no emission. To solve this problem and to increase VCSEL output power, as well as to improve its thermal characteristics, we develop a new type of injected VCSEL with a larger aperture and a reticular electrode, where the conventional circular injection electrode of the P side is turned into a reticular one, and the heat sink is on the N side. The tests of the new VCSEL show an improvement in homogeneity in not only the injected current but also the emission intensity. The optical output power is also considerably increased, and the device optoelectronic performance is improved.

OCIS codes: 140.0140, 140.7260, 250.7260, 140.5960.

doi: 10.3788/COL20100808.0773.

In recent years, in-depth investigations on the vertical-cavity surface-emitting laser (VCSEL) have facilitated the successful development of a high-power VCSEL. The enlargement of the emitting aperture is usually one of the important methods of increasing VCSEL optical output power. Although the output power is increased, the carrier conglomeration effect makes the injected carriers conglomerate in a ring near the aperture circumference when the active region diameter is greater than about 10 μm[1]. The current intensity at each point of the emission aperture is distributed inhomogeneously. It is greater near the circumference than that at about the center. At the same time, the larger apertures are due to the higher temperature around the aperture circumference[2−4] than that at the center in the laser device. This results in a weaker or even no emission at around the center, which deteriorates the characteristics of the device.

The near field patterns of the VCSEL with different active region diameters from 10 to 50 μm are shown in Fig. 1[5]. The homogeneity in optical output power is affected in the larger aperture VCSEL, so the carrier conglomeration effect has to be eliminated[6].

Considering the above reasons, in this work, we adopted a structure with a larger aperture and reticular electrode, which substitutes for the conventional one in order to address the problem of inhomogeneity in the injected current. The new device structure, as a high-power VCSEL, was emitted from the P side, and the heat sink was placed on the N side. A reticular electrode instead of the conventional circular electrode was placed on the P side of the device. The high-power reticular electrode VCSELs with a 400-μm-diameter aperture were fabricated using the above-mentioned techniques on the epitaxial side. The characteristics of the high-power VCSEL were tested in the experiments. Compared with the conventional VCSEL, the test results of our proposed VCSEL showed improvement in homogeneity in not only the injected current but also the emission intensity. At the same time, the optical output power was also increased, and the device optoelectronic performance was improved.

In the VCSEL with larger aperture, the inhomogeneity in the injected current often causes inhomogeneous or even no emission[7]. In order to solve this problem and increase VCSEL output power, we developed an injected VCSEL, where the conventional circular injection electrode (Fig. 2(a)) of the P side was turned into a reticular electrode (Fig. 2(b)), and a heat sink was placed on the N side. A Ti-Pt-Au alloy was evaporated on the P side to form a P-type reticular electrode, and two soldering trays were connected to it. A Ge-Au-Ni alloy was evaporated on the N side to form an N-type electrode.

The current of the conventional electrode VCSEL was injected through the circular electrodes. The ring trench between the circular electrodes and the ring leading electrodes acted as the oxidation window. However, the new structure with a reticular electrode is made of a larger round aperture at the center and outer smaller apertures surrounding it. Each openning is a channel of the injected current. The special features of the new structure are the channels of the injected current, which are homogeneously in the ring trench, and its two sides surrounded by the area of oxidation confinement. These channels were distributed homogeneously. The area of

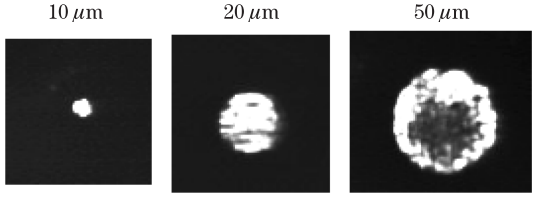

Fig. 1. Near field patterns of the VCSEL with different active region diameters.

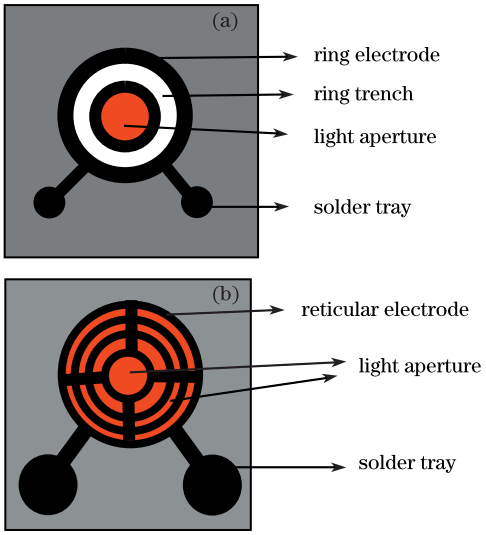

Fig. 2. Sketches of the two structures of VCSEL. (a) Conventional circular electrode of P side and (b) reticular electrode of P side.

oxidation confinement is located in the high aluminium layer in the distributed Bragg reflector (DBR). Compared with conventional structures, the material advantages of the new structure are as follows. Firstly, each independent smaller aperture is distributed in the whole area of the injected current, thereby eliminating the carrier conglomeration effect. Secondly, all apertures for the injected current are also in the area of emitted light, and accordingly, its intensity is distributed more homogeneously. Thirdly, this new type of VCSEL achieves heat dissipation because each aperture is comparted by the ring trench and oxidation confinement area. According to the above analyses, therefore, the device with a new structure not only improves the homogeneity in the injected current but also increases its output power.

The epitaxial wafer of VCSEL was grown on an N-type GaAs substrate using molecular beam epitaxy (MBE). The active layer contains three GaAs-AlGaAs quantum wells. N-DBR consists of 41 pairs of $Al_{0.22}Ga_{0.78}As/GaAs$, while P-DBR consists of 22 pairs of $Al_{0.22}Ga_{0.78}As/GaAs$. There is a 35-nm-thick $Al_{0.98}Ga_{0.02}As$ layer located at the first pair in P-DBR in order to form buried $AlGaAs/Al_xO_y$. The top layer is a GaAs contact layer. The whole epitaxial wafer thickness is about 650 μm, and the center wavelength of the DBR reflection spectrum is 808 nm. The photolithographic technique and wet chemical etching were used to form the oxidation window (Fig. 2) with an etched depth of 4.5 μm. The epitaxial wafer was oxidized at 420 °C with nitrogen carrier gas for 40 min. This layer was oxidized and converted to Al_xO_y later in the fabrication process for current and optical confinements. Then, a thin Al_xN_y[8] passivation layer was coated on the wafer, and an electrode window formed through secondary photolithography was opened to evaporate the Ti-Pt-Au alloy and form the P-type electrode. A Ge-Au-Ni alloy was evaporated to form an N-type electrode. Finally, the N-side of the cleaved chip was soldered onto a diamond heat sink to form the new device.

The devices were tested under continuous wave operation. The light power-current-voltage (P-I-V) characteristics of VCSEL at room temperature for two structures are shown in Fig. 3. The maximal power conversion efficiency (PCE) of VCSEL with a reticular electrode is up to 35%. From the V-I characteristic curve of VCSEL with a new structure, a differential resistance of 2 Ω and a slope efficiency of 0.75 mW/mA are obtained. From the P-I characteristic curve at room temperature, the device with a 400-μm aperture has a threshold current of 80 mA. A maximal output power of up to 410 mW at 650 mA, 1.5 times higher than that of the conventional electrode device, is realized. The test results of the new VCSEL show that its optoelectronic characteristics are better than those of the conventional device.

The whole resistance of VCSEL is the sum of the two parts of resistance for a top emitting structure, with a P-DBR as the output aperture[9,10]:

$$R_{\rm s} = R_{\rm l} + R_{\rm v} = \frac{\rho_{\rm inf}}{2\pi r_{\rm a}} + \frac{\rho_0}{\pi r_{\rm a}^2}, \tag{1}$$

where $R_{\rm s}$ is the total sum of resistance, $R_{\rm l}$ is the lateral and contact resistance (scales inversely with aperture perimeter), $R_{\rm v}$ is the vertical current flow resistance (scales inversely with aperture area), $r_{\rm a}$ is aperture radius, $\rho_{\rm inf}(\Omega \cdot {\rm cm})$ is the resistivity in lateral and contact resistance, and $\rho_0(\Omega \cdot {\rm cm}^2)$ is the resistivity in vertical current flow resistance.

According to Eq. (1), lateral and contact resistance is a limitation factor of the PCE. The structure with reticular electrode, however, makes the two parts of the resistance decrease. Moreover, the reticular apertures act as smaller homogeneous current channels, the aperture perimeter and area augment with increasing $r_{\rm a}$, so $R_{\rm l}$ and $R_{\rm v}$ are reduced.

The expression of power conversion efficiency is given by

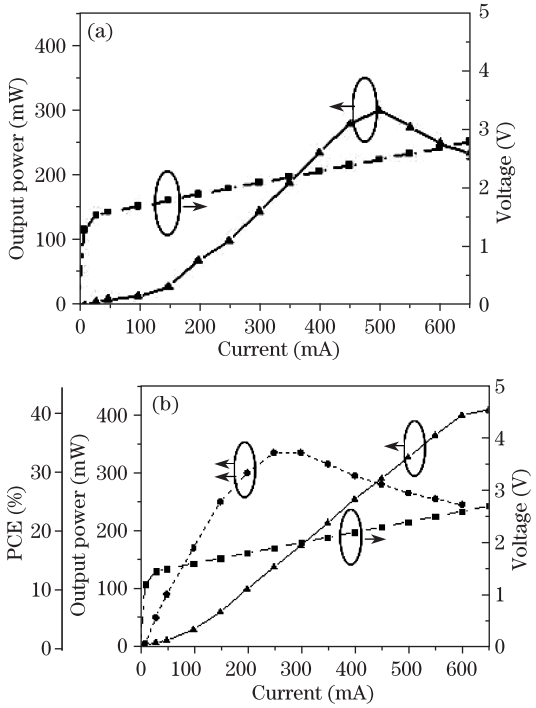

Fig. 3. P-I-V characteristic curves of VCSEL for (a) conventional structure and (b) new structure.

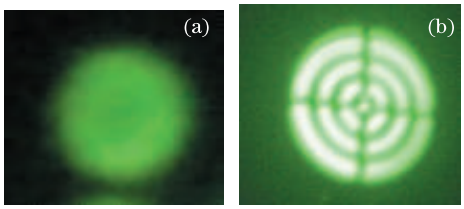

Fig. 4. Near field patterns of VCSEL for (a) conventional structure and (b) new structure.

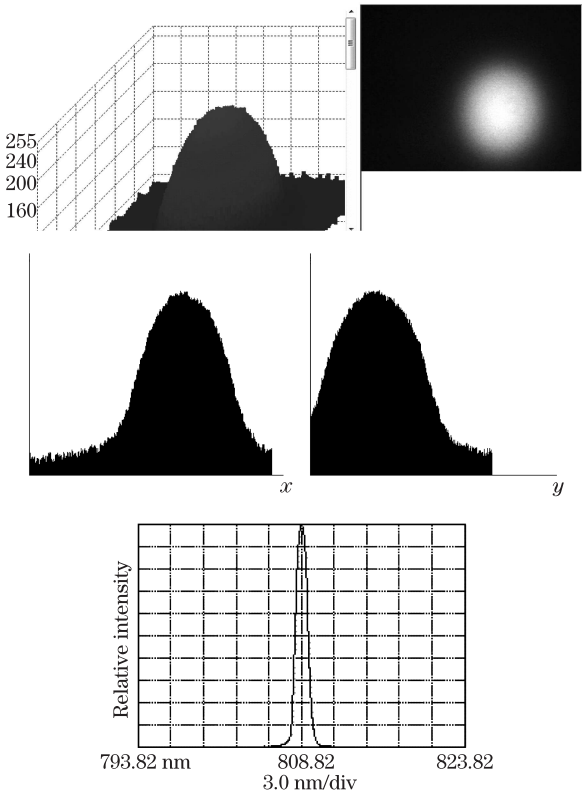

Fig. 5. Far field distribution and spectrum of the new structure of VCSEL.

$$\eta = \frac{P_{\mathrm{w}}}{IV + I^2 R_{\mathrm{s}}}, \tag{2}$$

where η is the power conversion efficiency, P_{w} is the actual output power of VCSEL, and $IV+I^2R_{\mathrm{s}}$ is theoretically the optical output power.

The decreased R_{s} leads to a diminished sum of the denominator, thereby increasing the power conversion efficiency. The results in Fig. 3 agree with the above-analyzed theories.

Figure 4 shows the near field patterns of VCSEL with the conventional and new structures, respectively. The emission area of the conventional strusture is of blemish, dispersed emission, and no emission in the dark area. The emission intensity of the whole device is insufficient and imperfect. However, the aperture emission with a new structure in the center and the other openings is homogeneous. Eliminating the previously inhomogeneous or no emission results, the new structure can cause the current to be injected into every emission area through the reticular electrode. This structure is suitable for the fabrication of VCSEL with a larger aperture. It also solves the problem in a larger emitting aperture in VCSEL, which leads to an inhomogeneous emission and a much weaker emission intensity at the center. At the same time, each single trench and aperture dissipates the heat and improves the device thermal performance.

The spectrum and far field pattern of VCSEL with a new structure are shown in Fig. 5. The central wavelength of 808.82 nm is obtained. The far field distribution is more homogeneous from the two-dimensional (2D) image. The device beam from the three-dimensional (3D) image shows Gaussian distribution and good beam quality.

In conclusion, a new type of injected VCSEL with a larger aperture and reticular electrode is fabricated, and its optoelectronic characteristics and output power are also tested. The test results show that the optical output power is increased, and the problem of inhomogeneity or even no emission is addressed. Moreover, there is an improvement in the beam quality, and the heat removal of the chips is more efficient. A slope efficiency of 0.75 mW/mA, an output power of up to 410 mW, and a peak power conversion efficiency of 35% are also presented.

This work was supported by the National Natural Science Foundation of China under Grant No. 60676025.

References

1. X. Li and J. Cheng, Transactions of Beijing Institute of Technology (in Chinese) **25,** 71 (2005).
2. T. Li, Y. Ning, Y. Sun, J. Cui, L. Qin, C. Yan, Y. Zhang, B. Peng, G. Liu, Y. Liu, and L. Wang, Chin. Opt. Lett. **5,** S156 (2007).
3. J. Cui, Y. Ning, T. Zhang, P. Kong, G. Liu, X. Zhang, Z. Wang, J. Shi, T. Li, L. Qin, Y. Liu, and L. Wang, Chinese J. Lasers (in Chinese) **36,** 1941 (2009).
4. T. Miyamoto, T. Nishina, Y. Kashihara, S. Ishida, and F. Koyama, Jpn. J. Appl. Phys. **47,** 6772 (2008).
5. J. Wu, H. D. Summers, and G. Iordache, in *Proceedings of CLEO 2001* CTuM22 (2001).
6. A. Mooradian, S. Antikichev, B. Cantos, G. Carey, M. Jansen, S. Hallstein, W. Hitchens, D. Lee, J.-M. Pelaprat, R. Nabiev, G. Niven, A. Shchegrov, A. Umbrasas, and J. Watson, in *Proceedings of MOC'09* M1 (2005).
7. T. Li, Y. Ning, Y. Sun, J. Cui, E. Hao, L. Qin, G. Tao, Y. Liu, L. Wang, D. Cui, and Z. Xu, Chinese J. Lasers (in Chinese) **34,** 641 (2007).
8. Z. Qiao, B. Bo, Y. Yao, X. Gao, J. Zhang, Y. Wang, C. Liu, P. Lu, H. Li, and Y. Qu, Chinese J. Lasers (in Chinese) **36,** 2277 (2009).
9. J.-F. Seurin, C. L. Ghosh, V. Khalfin, A. Miglo, G. Xu, J. D. Wynn, P. Pradhan, and L. A. D'Asaro, Proc. SPIE **6908,** 690808 (2008).
10. K. L. Lear, S. P. Kilcoyne, and S. A. Chalmers, IEEE Photon. Technol. Lett. **6,** 778 (1994).